SSRG International Journal of Electrical and Electronics Engineering
ISSN: 2348-8379/ https://doi.org/10.14445/23488379/IJEEE-V10I8P119

Volume 10 Issue 8, 195-205, August 2023

Original Article

Design and Implementation of 85dB CMRR, 4.2 MHz CMOS Instrumentation Amplifier for Bio-Electric Signals

Milind P Gajare[1], Dnyandeo K Shedge[2], Mohini P Sardey[3], Vinayak K Bairagi[4]

[1,2,3,4]*Electronics and Telecommunication Engineering Department, AISSMS Institute of Information Technology, Pune, India.*

[1]*Corresponding Author : milind.gajare@assmsioit.org*

Received: 19 June 2023 Revised: 23 July 2023 Accepted: 15 August 2023 Published: 31 August 2023

Abstract *- This paper presents the design and Implementation of a novel CMOS Instrumentation Amplifier using capacitive neutralization and feedback transconductance techniques for bioelectric signal enhancement. The proposed amplifier also implements indirect current feedback, operating at a 3-volt supply. With a compact footprint of 0.062mm² on the chip, the amplifier achieves an impressive bandwidth of 4.2MHz and 85 dB CMRR. Implemented using 0.25µm CMOS technology, the proposed Instrumentation Amplifier showcases notable characteristics.*

Keywords *- Bandwidth, Bioelectric signals, CMRR, ICMR, Indirect current feedback, Power consumption.*

1. Introduction

Electrical signals produced by human beings are known as bioelectric signals. These signals are created by the electrical activity of cells that use electricity to interact with one another, such as neurons and muscle cells [1]. The flow of ions across the cell membrane in neurons produces bioelectric signals by generating an electrical potential difference between the interior and outside of the cell.

An action potential, a brief burst of electrical activity that travels down the length of the neuron, can be produced when a neuron receives a signal from another neuron [2]. This action potential can cause the release of neurotransmitters at the synapse, the location where the neuron connects with another neuron or a muscle cell. Depending on the signal type and the body's location being monitored, bioelectric signals can be measured using various methods [3]. The frequency ranges of such bioelectric signals vary from DC to a few hertz, and the amplitude of bioelectric signals varies from almost zero voltage to a few microvolts [4]. Bioelectric signals play an essential part in the operation of living organisms and are important in many fields of healthcare and biomedical research [5, 6]. Bioelectric signals are necessary for the body's healthy functioning, diagnosis, monitoring, and healthcare and biomedical research advances. They provide significant information about an organism's physiological status and contribute to developing novel medical technologies and therapies. The most popular methods for monitoring bioelectric signals are listed below:

1.1. Electroencephalography (EEG)

This method uses electrodes on the scalp to analyse the brain's electrical activity. EEG is used to identify neurological disorders, brain activity, and cognitive processes.

1.2. Electromyography (EMG)

This method uses electrodes implanted into or applied to the skin to measure the electrical activity of muscle cells. EMG is used to identify neuromuscular conditions, investigate muscle activity, and conduct biomechanics research.

1.3. Electrocardiography (ECG)

This method uses electrodes on the chest, arms, and legs to measure the heart's electrical activity. Cardiologists utilize ECG to identify cardiac problems, track heart health, and conduct research.

1.4. Electrooculography (EOG)

This method is used to gauge the electrical activity of the eye-moving muscles. In order to detect changes in electrical potential when the eyes move, the technique entails putting electrodes close to the eyes, often on the forehead and around the eyes.

1.5. Electroretinography (ERG)

A method for determining how electrically active the retina is in response to light stimulation is called Electroretinography (ERG). In order to detect changes in

electrical potential as light is given to the eye, the approach entails putting electrodes on the cornea and around the eye. The amplitude and frequency of such bioelectric signals are also quite low [5]. A summary of the characteristics of bioelectric signals is represented in Table 1. Bioelectric signals are time-varying voltage signals. These signals are recorded by mounting multiple electrodes on or into the human body. Mathematically, these signals are expressed as:

$$X(n) = f(n\Delta t) \quad (1)$$

Where Δt is the sampling interval of the signals and $f(n\Delta t)$ is the signal's voltage at time Δt.

It is observed that the bioelectric signal acquisition system consists of Electrodes that detect bioelectric signals and an Instrumentation Amplifier (IA) that amplifies signals. This filter removes noise and Analog to Digital Converter (ADC), which converts the signal into a digital signal [21, 22]. Bioelectric signals picked up by electrodes are usually fragile; for faithful amplification with noise cancellation of such signals, an Instrumentation amplifier is always a perfect choice for researchers. It has been observed that the interferences frequently accompany the bioelectric signals.

In many applications, monitoring a weak signal at high frequencies is desirable while still experiencing significant standard mode noise [27]. Such signal conditioning circuits must be compact, portable, and battery-operated in biomedical applications.This necessitates the need for an Instrument Amplifier (IA) with a smaller size, lower power consumption, higher Common Mode Rejection Ratio (CMRR), and extended frequency.

IA factors like CMRR, bandwidth, Input Common-Mode Range (ICMR), power dissipation, output voltage swing, and chip size significantly impact how well frontend systems perform [3]. Three op-amp topologies and current feedback are different topologies used to design IA [4-19]. This research focuses on methods for enhancing IA parameters like bandwidth, power, and size. This work aims to comprehend the indirect current feedback on IA's planning, implementation, optimization, and testing processes [23].

Table 1. A summary of the characteristics of bioelectric signals

Signal Type	ECG	EEG	EMG	EOG	ERG
Source of signal	Heart	Brain	Muscles	Eye movements	Retina
Amplitude	Microvolts	Microvolts	Millivolts	Millivolts	Microvolts
Frequency	0.05 -100Hz	0.5-100Hz	20-500Hz	0.1-10Hz	0.1-100Hz
Main waveform	P, QRS,T	Alpha, Beta, Theta, Delta	N/A	N/A	A, B, C,D waves
Purpose	Cardiac function	Study brain activity	Muscle activity	Eye movement tracking	Retinal function diagnosing
Application	Diagnosing heart conditions, detecting arrhythmias	Sleep analysis, Cognitive research	Assessing muscle function, detecting abnormalities	During sleep studies, ocular disorders	Retinal function disorders

Various sensors are used to detect bioelectric signals. The disadvantage of sensor output is that it is always less in amplitude, accompanied by common-mode solid noise. To amplify such weak signals with noise rejection capabilities, Instrumentation Amplifiers (IA) are always preferred by researchers.

Therefore, developing an IA that is compact, wide-band and uses little power is necessary. The crucial IA factors that influence how well frontend systems work are Power Consumption (µW), Bandwidth (BW), Common Mode Rejection Ratio (CMRR), Input Common Mode Range (ICMR), and chip area. Three op-amps IA and current feedback IA are examples of different topologies utilized in IA design [1, 2]. For designing the IA, the three op-amp topology quickly gained popularity [2]. A creative adaptation of the buffered subtractor circuit is the traditional 3-op amp IA circuit [16-20]. The output subtractor stage tends to cancel out common mode mistakes in the input stages if they occur concurrently because of the symmetry of this structure. This includes frequency-dependent mistakes like common-mode rejection. These characteristics make this setup well-liked.

Building 3-op amp instrumentation amplifiers can be done using a bipolar or a FET-based op-amp topology. Due to their shallow bias currents, FET input op-amps are typically well-suited for usage with sources with high impedance values ($>10^6$). The topology IA with resistive feedback is the foundation of every research [31]. Additionally, they offer a higher slew rate for a given power level. It has been observed that the three op-amp

CMRR offset voltages are often lower and more significant for FET amplifiers [28, 30]. Compared to BJT amplifiers, FET amplifiers often have lower CMRR, higher offset voltage, and higher offset drift.

By reviewing the work done so far by the researchers, it is observed that Input Common Mode Rejection Ratio (ICMR), Common Mode Rejection Ratio (CMRR), Bandwidth (BW), Power Consumption, Total input noise and area of the chip are essential parameters for the acquisition of bioelectric signals. Various methodologies are implemented to build a CMOS-based Instrumentation amplifier. These methodologies, along with applications, are tabularized in the table below.

Table 2. Parameters, methodologies and applications of various bioelectric signal acquisitions

Ref. No.	ICMR	Bandwidth	CMRR (dB)	Power Consumption	Input Referred Noise (µv)	Area (mm^2)	Methodology	Application
[1]	±4.5 V	N/A	99	500µw	1.4 µv	24	Current Feedback	ECG
[2]	±5mV	200Hz	100	9µw	6 µv	N/A	Current Balancing	ECG
[6]	1V	2KHz	N/A	1.55 µW	0.7µv	N/A	Current Balancing	Bio Impedance
[7]	1V	1.1KHz	125	2.3 µW	2.18 µv	N/A	Chopper Stabilized	EEG
[8]	3.3 V	N/A	N/A	11.8mW	N/A	N/A	Current Feedback	EIT
[9]	N/A	2MHz	100	634 µW	15.7µv	0.111	Current Feedback	Bio Spectroscopy
[11]	N/A	N/A	N/A	24 µW	35nv	2.8	Dual Path	Bio Impedance
[12]	0.5V	250Hz	90	1.3 µW	2.8µv	N/A	Capacitive Coupled	Wireless Body Area Network
[13]	1.8V	N/A	100	N/A	0.78µv	N/A	Fully Differential	ECG, EEG, EMG,EOG
[14]	1.6V	2MHz	90	9.9mW	16.4µv	N/A	CFIA using Neutralization Capacitor	Bio Impedance Spectroscopy
[15]	3.3V	125Hz	125	132 µW	2.3µv	N/A	Current Balanced	Wearable Physiological Monitoring
[17]	1 V	N/A	125	165 µW	3.192µv	N/A	Folded Cascode	ECG
[18]	1V	256Hz	104	N/A	1.51µv	N/A	Fully Differential Chopper Current Balancing	ECG,EEG, EMG, EOG
[19]	N/A	150Hz	83.24	672	2.01µv	0.071	DDA-Based Fully-Differential	ECG
[20]	N/A	170Hz	120	840	0.0182µv	0.0736	Current Feedback	ECG,EEG

A thorough literature analysis suggests that various alternative design methodologies can be used for CMOS IA. The performance of many biomedical measurement systems is constrained by the analogue frontend circuit employed for signal conditioning. A typical frontend circuit, the CMOS IA, has a high CMRR, a large bandwidth, and a manageable size for portability [26]. Researchers are looking into novel design strategies for CMOS IA that will reduce power consumption, boost CMRR and bandwidth, and reduce chip space. To evaluate the weaker biological signals accompanied by common mode noise, the CMRR and bandwidth can be improved in various methods. To enhance the CMRR, a modern feedback approach is employed.

It is observed that segregation and balancing techniques provide high CMRR. Two MOSFETs on the same branch carry different currents in direct current feedback; this results in nonlinearity and reduces the input common-mode voltage range. In indirect current feedback, nonlinearity is eliminated since MOSFETs on the input and output sides carry equal currents [24, 25]. Additionally, while at a higher cost in terms of power consumption, the ICMR voltage is enhanced.

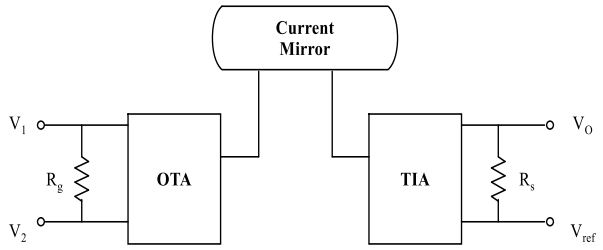

Fig. 1 Block diagram of current feedback instrumentation amplifier

According to the research done on CMOS IA, The CMRR, bandwidth, and power savings of Indirect Current Feedback (ICF) architecture with CMOS devices will be significantly enhanced [24]. The essential functional block diagram representation is shown in Figure 1. It uses Input transconductance (V to I converter) and output as a transimpedance (I to V converter) amplifier. The same current is mirrored in this configuration's input and output branches. As a result, using improved tactics previously advised to operate the MOSFET in the triode region, it has been determined to employ this strategy in this study to optimise the CMRR and bandwidth further.

2. Materials and Methods

The block diagram of the proposed IA using the current balancing, isolation, and indirect current feedback techniques is shown in Figure 2. The input stage amplifier of a differential transconductance functions as a buffer amplifier. Instead of using a resistor load, this transconductance amplifier is loaded by a current mirror source. This current mirror source has high local loop gain and high output impedance. Due to the reduced parasitic poles in the loop, stability with broad bandwidth operation is a benefit. A balanced differential amplifier with high gain serves as a sensing amplifier and makes up the second stage in a block diagram [30].

The first and second stages of the planned IA will reduce the majority of the common mode noise. To balance their drain currents, the output voltage of this stage will be provided to the trans-impedance amplifier, forcing the input and output voltages across the resistors that determine the gain of IA.

The first three stages determine the maximum gain of the IA. The next stage is the telescopic Cascode amplifier, which offers low gain [29]. Therefore, the diode-connected load can load this step. A second transconductance amplifier with a capacitor filter is introduced as feedback from the output to the cascade op-amp to remove the undesired low-frequency interference. This stage determines the 3 dB frequency of IA.

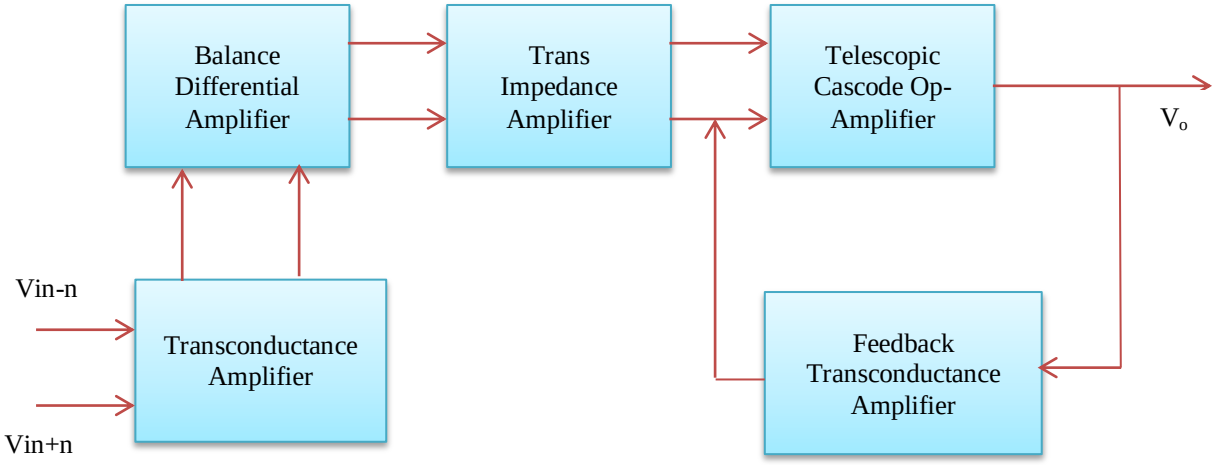

Fig. 2 Block diagram of proposed IA

3. Results and Discussion

The proposed Instrumentation Amplifier (IA) operates through a meticulous five-stage process, each undergoing individual simulation to achieve the desired outcomes. Once the optimal results are attained, the Comprehensive Instrumentation Amplifier is meticulously constructed by seamlessly integrating all stages. The operational requirements are met by implementing a 3 V power supply. The amplifier is subjected to an input signal with an amplitude of 100µV while carrying a current of 38µA, ensuring efficient energy utilization at a mere 794 µW power consumption. The IA boasts a bandwidth of 4.2 MHz to accommodate a broad frequency range. Significantly, the IA's performance is marked by an impressive Common-Mode Rejection Ratio (CMRR) of 80-90 dB, attesting to its exceptional capability to differentiate between desired signals and unwanted noise.

3.1. Input Transconductance Amplifier Design

ECG, EEG and EMG signals are characterized by low amplitudes in the microvolt (µV) range and low-frequency components. Due to their small amplitudes, the transistors used in the readout frontend circuits must operate in the frequency domain where 1/f noise is most prominent. PMOS transistor offers lower flicker noise, acting as an input transistor for IA. This type of noise, also known as pink noise, increases as the frequency decreases, posing a significant challenge for signal amplification and processing. The proposed circuit for CMOS IA's input stage is the Operational Transconductance Amplifier (OTA), which determines noise interference. Thermal noise trumps the above flicker as the bandwidth of IA approaches 4.2 Mega Hertz. As a result, the IA input-referred noise can be calculated as

$$\frac{\mathbf{V}_{iN}^2}{\Delta f}=4kTR_1+2\left(4kT\frac{2}{3}\frac{1}{g_{mi1,2}}+4kT\frac{2}{3}\frac{g_{md1,2}}{g_{mi1,2}^2}\right) \qquad (2)$$

T is the absolute temperature in degrees Kelvin, k is the Boltzmann constant, and f is the noise evaluation bandwidth in Hz. To limit the thermal noise addition, resistor R_1 is chosen to be of low value. The PMOS transistors are used as input transistors to minimize 1/f noise; using a Trans conductance amplifier at this stage can remove noise and enhance the bandwidth of the IA.

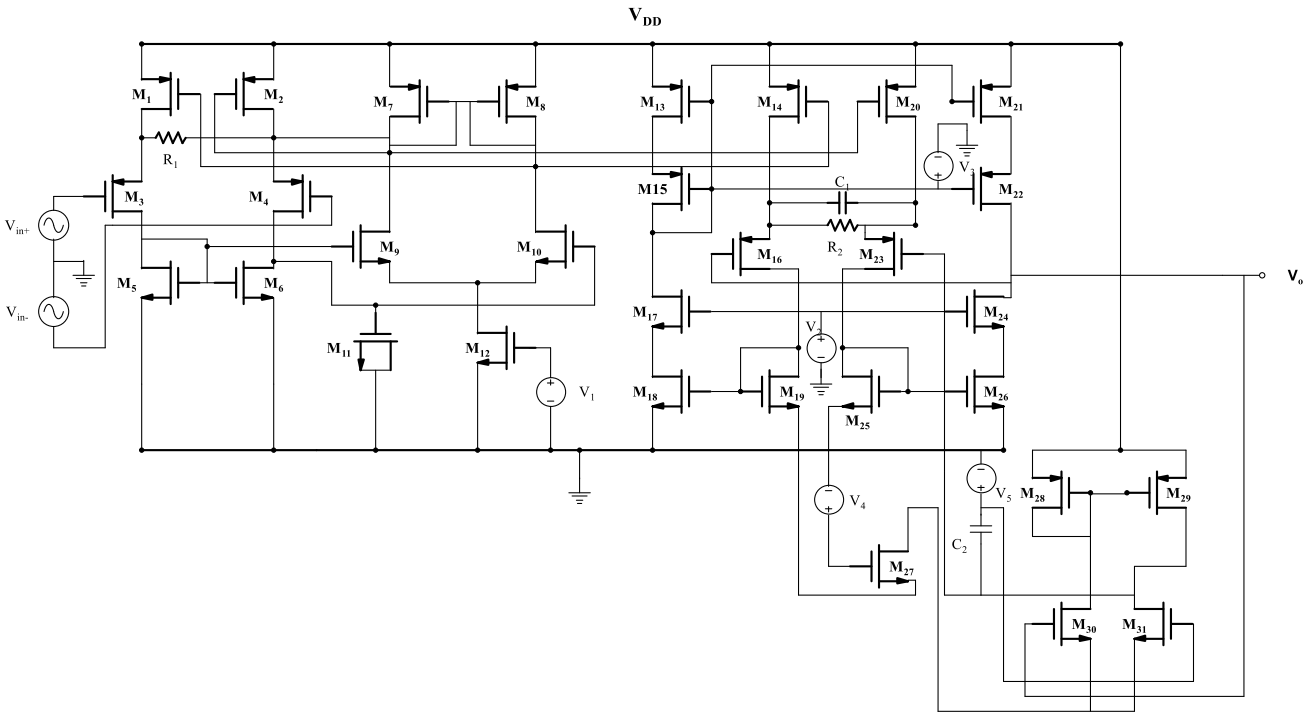

Fig. 3 Circuit diagram of the proposed instrumentation amplifier

The Operational Trans conductance amplifier of this stage offers high gain for the Instrumentation amplifier. In the transconductance stage, the input transistors M3 and M4 convert the differential input voltages, vin- and vin+, into current I_1. As the amplifier is designed to be balanced, the small signal current I_1 passes through the resistor R_1. To mirror this current, current mirrors M_{14} and M_{20} are employed in the trans-impedance stage, where the current I_2 flows through resistor R_2 and generates an output voltage. The dimensions of input MOSFETs are considered as 330:3 µm. Source network dimensions are 200:2.5, and the drain network is considered as 12:5.

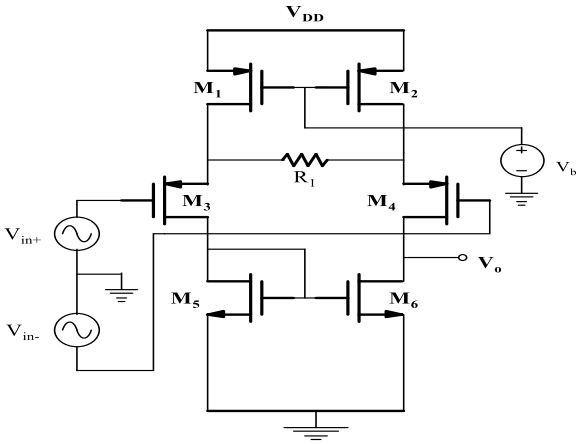

Fig. 4 Input transconductance amplifier

3.2. Differential Amplifier Design

A Differential amplifier with a balanced output circuit is implemented for this stage. When no signal is provided, the circuit is fully balanced and differential; thus, all currents are equal and v_{out} = 0; for this stage, a connected differential amplifier is considered. Input MOSFETs of this stage are considered as 300:3. Dimension for the current mirror biasing network is considered as 100:2.5. Source network dimensions are taken as 200:5. A Neutralization capacitor using 17.8:5 dimensions is used in this stage for better bandwidth of the amplifier.

3.3. Operational Transimpedance Amplifier Design

For this stage, an Operational Trans impedance Amplifier is implemented, similar to the input stage A CMOS OTA and cascode single-ended differential amplifier make-up.

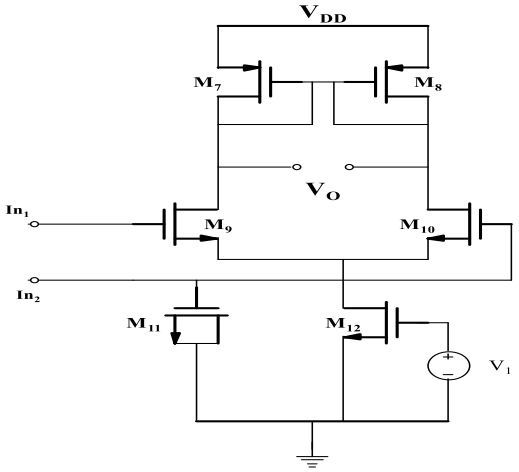

Fig. 5 Differential amplifier

For this equation we have considered $(W/L)_9 = 2.5 (W/L)_7$. The output stage, Dimensions of PMOS are 100:1, and of NMOS are 40:1.

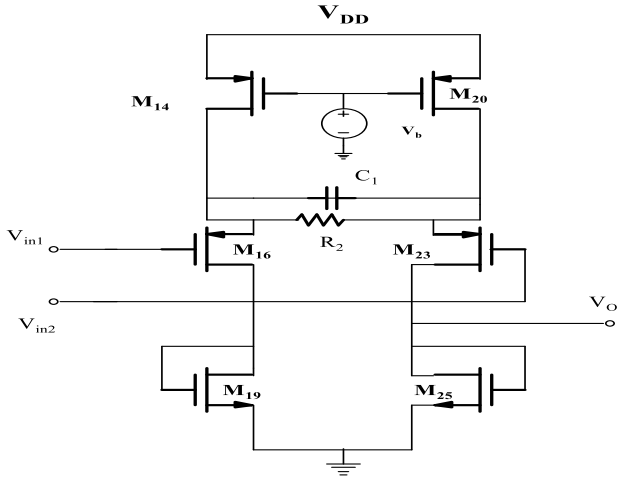

Fig. 6 Transimpedance amplifier

The resistors R2 and C2 decide the amplifier's high cutoff frequency.

3.4. Telescopic Cascode Operational Amplifier Design

The output voltage swing technique implements the telescopic cascode operational amplifier. For Implementation, PMOS are considered as 80:1 and NMOS are considered as 40:1

3.5. Output Transconductance Amplifier Design

This stage Transconductance amplifier is designed along with an order high pass filter to remove low-frequency connected to the human body to acquire bioelectric signals. Instead of using V_{ref}, this filter is incorporated into a feedback path created between the output terminal and one of the input terminals of the output OTA. According to the block diagram of the proposed IA, the high-pass filter is implemented by a straightforward operational transconductance amplifier with transconductance Gm and a capacitor C_2.

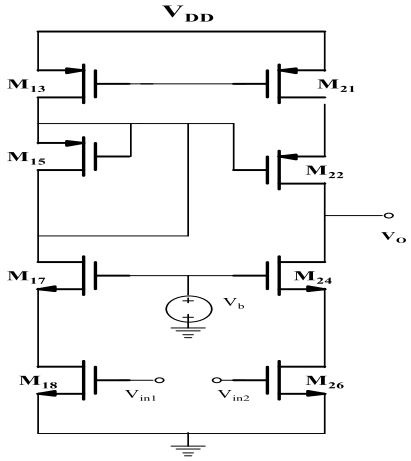

Fig. 7 Telescopic cascode amplifiers

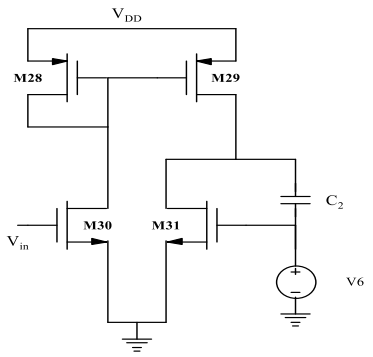

Fig. 8 Feedback transconductance amplifier

All the above stages are interconnected to build a complete Instrumentation amplifier. The frequency response of the proposed amplifier is observed. By running some of the devices in the triode region rather than saturation, the bandwidth of this stage can be enhanced by 4.2 MHz.

The other parameters measured are power dissipation of 794µW, CMRR of 85 dB, chip area of 0.062 mm^2, and input referred noise of 36 µVrms. The CMRR is marginally reduced, the power dissipation is decreased, and the bandwidth is raised. The circuit is simulated for various bioelectric signals, and output is observed. Table 3 compares recently published work with newly proposed work.

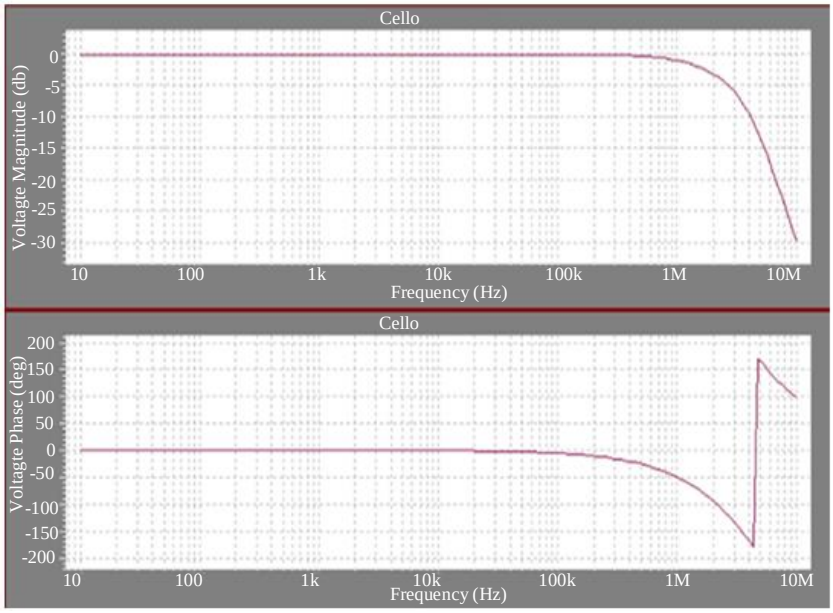

Fig. 9 Frequency response of instrumentation amplifier

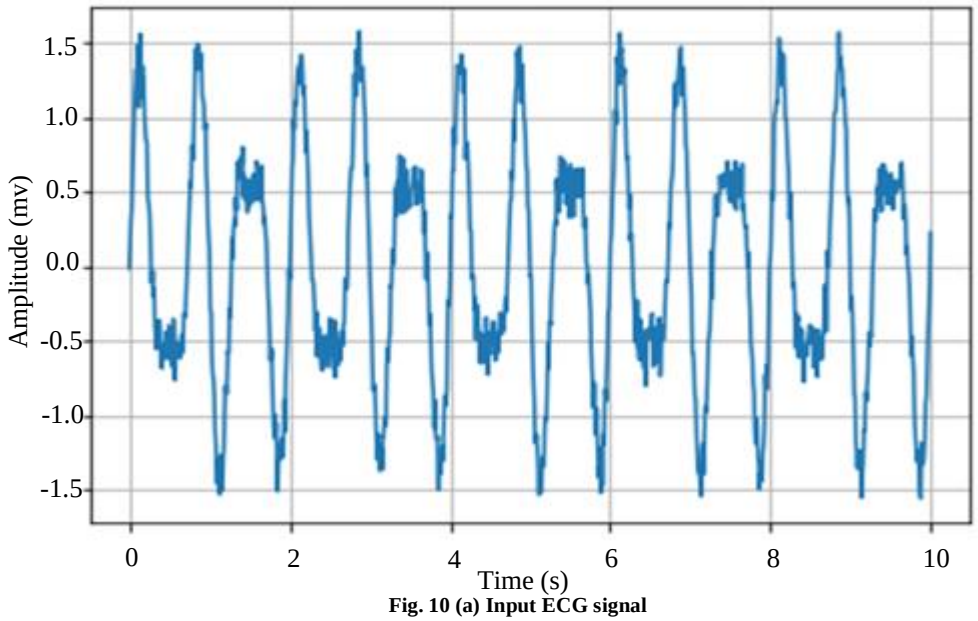

Fig. 10 (a) Input ECG signal

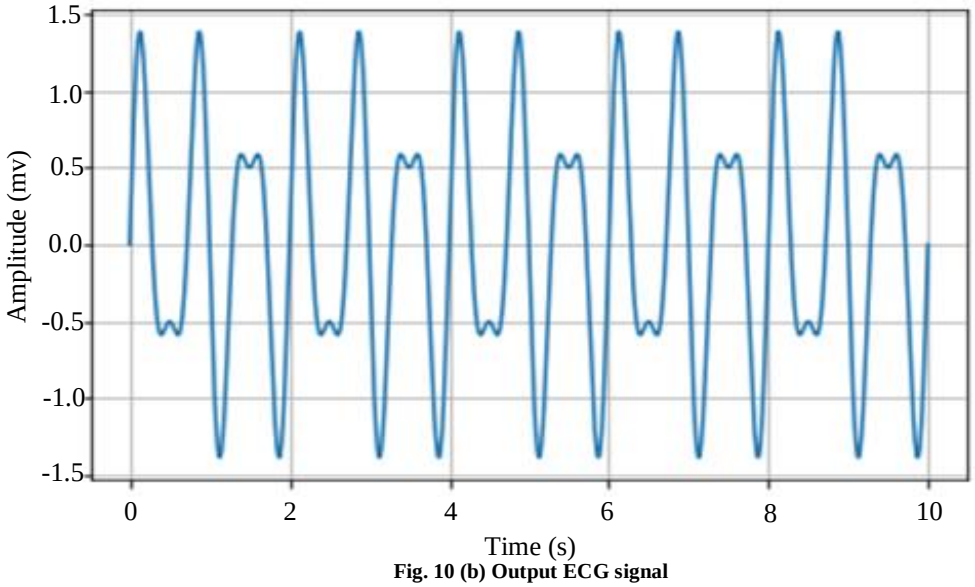

Fig. 10 (b) Output ECG signal

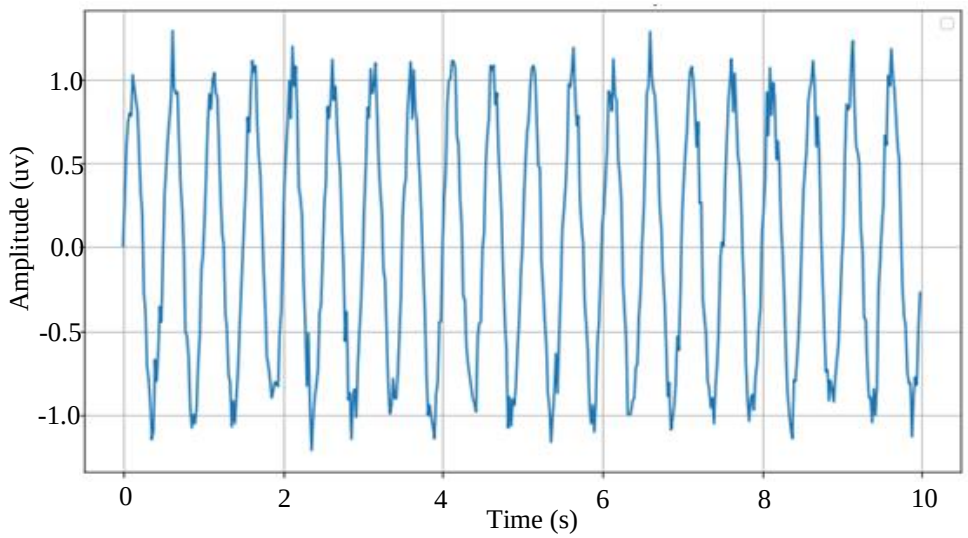

Fig. 11 (a) Input EEG signal

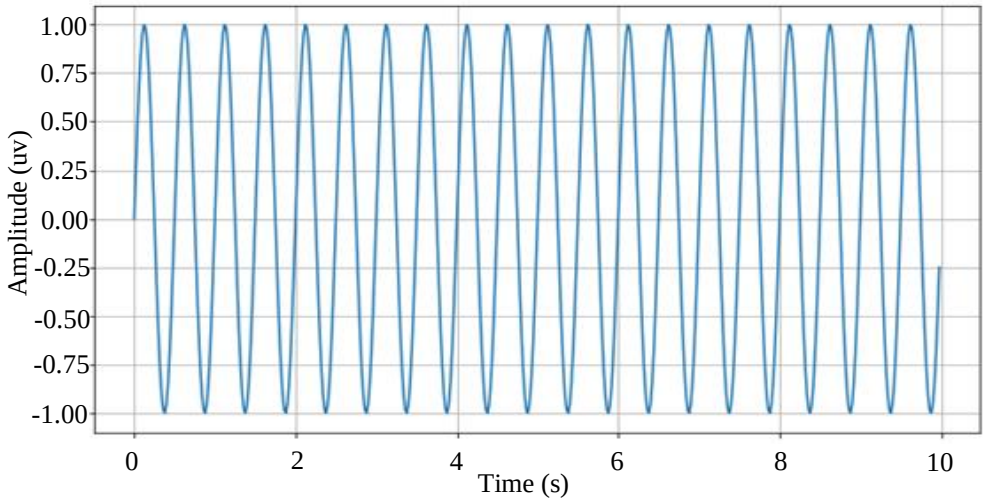

Fig. 11 (b) Output EEG signal

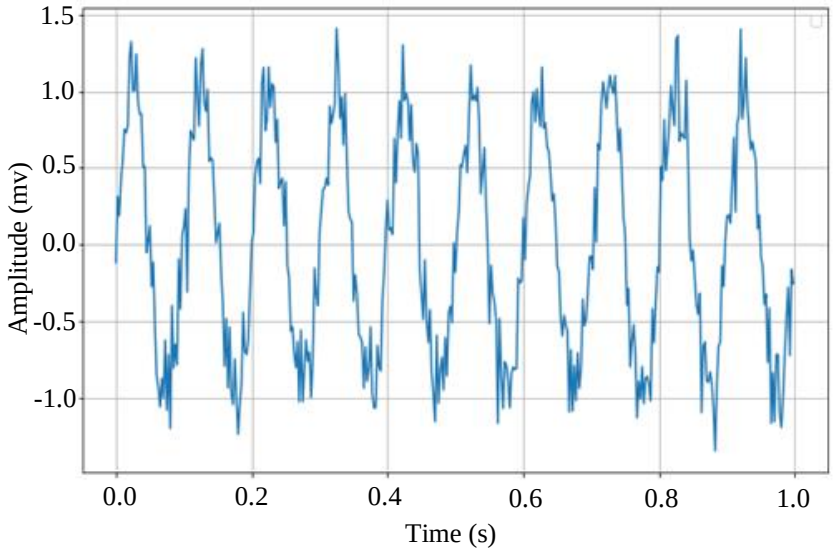

Fig. 12 (a) Input EMG signal

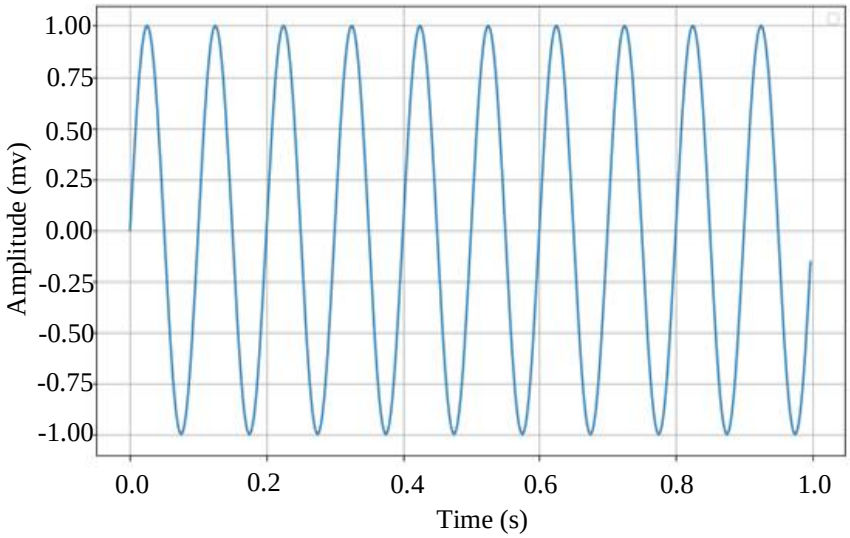

Fig. 12 (b) Output EMG signal

Table 3. The measured performance parameters of the instrumentation amplifier

Parameters	This Work	2019 [7]	2011 [14]	2021 [19]	2021 [20]	2023 [31]
Application	ECG/EEG/ EMG	EEG	EIT	ECG	ECG/EEG	ECG
Technology (µm)	0.25	0.13	0.35	0.35	0.18	0.18
Active area (mm^2)	0.062	N/A	0.068	0.071	0.0736	0.0167
Voltage (V)	3	1	3	2	1.8	0.5
Power consumption (µW)	794	2.3	870	672	840	0.0313
Input referred noise (µv)	36	2.18	16	2.01	0.0182	17.9
Gain	50	N/A	50	N/A	N/A	37.1
CMRR (dB)	85	125	90	83.24	120	75
Bandwidth	4.2MHz	1.1KHz	2MHz	150Hz	170Hz	112Hz

4. Conclusion

This study presents the Implementation of an Instrumentation Amplifier (IA) utilizing the indirect current feedback topology. A novel technique is employed to operate the MOSFET in cascode current mirror load within the telescopic cascode op-amp, positioned at the edge of the triode region. The performance of the IA for bioelectric signals is evaluated through simulation using the Cadence EDA tool. The system operates at a supply voltage of 3 volts to ensure low power consumption.

The MOSFET quiescent currents are carefully selected to achieve a power dissipation of 794 µW while maintaining a bandwidth of 4.2 MHz. The results obtained from the simulations demonstrate the successful Implementation of the Instrumentation Amplifier for amplifying bioelectric signals.

The chosen operating conditions, including the supply voltage and MOSFET quiescent currents, yield the desired power dissipation and bandwidth. In conclusion, this study successfully implements an Instrumentation amplifier for bioelectric signals using capacitive neutralization and feedback transconductance amplifier.

The IA's performance is evaluated through simulation, and it achieves the desired Common Mode Rejection Ratio and bandwidth requirements. This research contributes to developing efficient amplification solutions for medical applications involving bioelectric signals.

References

[1] R. Martins, S. Selberherr, and F. A. Vaz, "A CMOS IC for Portable EEG Acquisition Systems," *IEEE Transactions on Instrumentation and Measurement*, vol. 47, no. 5, pp. 1191-1196, 1998. [CrossRef] [Google Scholar] [Publisher Link]

[2] Maryam Shojaei-Baghini, Rakesh K. Lal, and Dinesh K. Sharma, "A Low-Power and Compact Analog CMOS Processing Chip for Portable ECG Recorders," *2005 IEEE Asian Solid-State Circuits Conference*, Hsinchu, Taiwan, pp. 473-476, 2005. [CrossRef] [Google Scholar] [Publisher Link]

[3] R. S. Khandpur, *Handbook of Biomedical Instrumentation*, 3rd ed., McGraw Hill Education (India) Private Limited, pp. 43-49, 2014. [Google Scholar] [Publisher Link]

[4] Viola Schaffer et al., "A 36 V Programmable Instrumentation Amplifier with Sub-20 µV Offset and a CMRR in Excess of 120 dB at All Gain Settings," *IEEE Journal of Solid-State Circuits*, vol. 44, no. 7, pp. 2036-2046, 2009. [CrossRef] [Google Scholar] [Publisher Link]

[5] Mohamad Rahal, and Andreas Demosthenous, "A Synchronous Chopping Demodulator and Implementation for High-Frequency Inductive Position Sensors," *IEEE Transactions on Instrumentation and Measurement*, vol. 58, no. 10, pp. 3693-3701, 2009. [CrossRef] [Google Scholar] [Publisher Link]

[6] Milad Zamani et al., "A 1.55 µW Bio-Impedance Measurement System for Implantable Cardiac Pacemakers in 0.18 µm CMOS," *IEEE Transactions on Biomedical Circuits and Systems*, vol. 12, no. 1, pp. 211-221, 2018. [CrossRef] [Google Scholar] [Publisher Link]

[7] Chung-Jae Lee, and Jong-In Song, "A Chopper Stabilized Current-Feedback Instrumentation Amplifier for EEG Acquisition Applications," *IEEE Access*, vol. 7, pp. 11565-11569, 2019. [CrossRef] [Google Scholar] [Publisher Link]

[8] Arun Rao et al., "An Analog Front End ASIC for Cardiac Electrical Impedance Tomography," *IEEE Transactions on Biomedical Circuits and Systems*, vol. 12, no. 4, pp. 729-738, 2018. [CrossRef] [Google Scholar] [Publisher Link]

[9] Elkyn Hernández Sanabria et al., "A Design Methodology for an Integrated CMOS Instrumentation Amplifier for Bioespectroscopy Applications," *2017 CHILEAN Conference on Electrical, Electronics Engineering, Information and Communication Technologies (CHILECON)*, Pucon, pp. 1-7, 2017. [CrossRef] [Google Scholar] [Publisher Link]

[10] Behzad Razavi, *Design of Analog CMOS Integrated Circuits*, 2nd ed., Tata Megraw Hill, pp. 124-126, 2017. [Google Scholar] [Publisher Link]

[11] Kwantae Kim et al., "A 24 µW 38.51 mΩrms Resolution Bio-Impedance Sensor with Dual Path Instrumentation Amplifier," *ESSCIRC 2017 - 43rd IEEE European Solid State Circuits Conference*, Leuven, Belgium, pp. 223-226, 2017. [CrossRef] [Google Scholar] [Publisher Link]

[12] Zhangming Zhu, and Wenbin Bai, "A 0.5-V 1.3- µW Analog Frontend CMOS Circuit," *IEEE Transactions on Circuits and Systems II: Express Briefs*, vol. 63, no. 6, pp. 523-527, 2016. [CrossRef] [Google Scholar] [Publisher Link]

[13] Devarshi Mrinal Das et al., "A Novel Low-Noise Fully Differential CMOS Instrumentation Amplifier with 1.88 Noise Efficiency Factor for Biomedical and Sensor Applications," *Microelectronics Journal*, vol. 53, pp. 35-44, 2016. [CrossRef] [Google Scholar] [Publisher Link]

[14] Apisak Worapishet, Andreas Demosthenous, and Xiao Liu, "A CMOS Instrumentation Amplifier with 90-dB CMRR at 2-MHz using Capacitive Neutralization: Analysis, Design Considerations, and Implementation," *IEEE Transactions on Circuits and Systems I: Regular Papers*, vol. 58, no. 4, pp. 699-710, 2011. [CrossRef] [Google Scholar] [Publisher Link]

[15] D. Susheel Kumar et al., "A High CMRR Analog Front-End IC for Wearable Physiological Monitoring," *2012 Annual IEEE India Conference (INDICON)*, Kochi, India, pp. 385-388, 2012. [CrossRef] [Google Scholar] [Publisher Link]

[16] M. P. Varghese, and T. Muthumanickam, "An Analog Circuit Designing Model via Machine Learning for Stage Classification and Evolutionary Solution Optimization Algorithm," *SSRG International Journal of Electronics and Communication Engineering*, vol. 10, no. 6, pp. 17-26, 2023. [CrossRef] [Publisher Link]

[17] Chinmayee Nanda et al., "A CMOS Instrumentation Amplifier with Low Voltage and Low Noise for Portable ECG Monitoring Systems," *2008 IEEE International Conference on Semiconductor Electronics*, Johor Bahru, Malaysia, pp. 54-58, 2008. [CrossRef] [Google Scholar] [Publisher Link]

[18] Wei-Chih Huang, and Kea-Tiong Tang, "A 90 nm CMOS Low Noise Readout Front-End for Portable Biopotential Signal Acquisition," *2012 IEEE Biomedical Circuits and Systems Conference (BioCAS)*, Hsinchu, Taiwan, pp. 33-36, 2012. [CrossRef] [Google Scholar] [Publisher Link]

[19] Chutham Sawigun, and Surachoke Thanapitak, "A Compact Sub-μW CMOS ECG Amplifier with 57.5-MΩ Zin, 2.02 NEF, 8.16 PEF and 83.24-dB CMRR," *IEEE Transactions on Biomedical Circuits and Systems*, vol. 15, no. 3, pp. 549-558, 2021. [CrossRef] [Google Scholar] [Publisher Link]

[20] Zaniar Hoseini et al., "Current Feedback Instrumentation Amplifier with Built-in Differential Electrode Offset Cancellation Loop for ECG/EEG Sensing Frontend," *IEEE Transactions on Instrumentation and Measurement*, vol. 70, pp. 1-11, 2021. [CrossRef] [Google Scholar] [Publisher Link]

[21] Cesar Augusto Prior et al., "Design of an Integrated Low Power High CMRR Instrumentation Amplifier for Biomedical Applications," *SBCCI '07: Proceedings of the 20th Annual Conference on Integrated Circuits and Systems Design*, pp. 71-75, 2007. [CrossRef] [Google Scholar] [Publisher Link]

[22] R. Carlo Novara, and Mohamed Djemai, "Design of a CMOS Multiplexer with Ultra Low Power using Current Mode Logic Technology," *SSRG International Journal of VLSI & Signal Processing*, vol. 3, no. 2, pp. 8-12, 2016. [CrossRef] [Google Scholar] [Publisher Link]

[23] R. F. Yazicioglu et al., "A 60μW 60nV/radicHz Readout Frontend for Portable Biopotential Acquisition Systems," *2006 IEEE International Solid State Circuits Conference - Digest of Technical Papers*, San Francisco, CA, USA, pp. 109-118, 2006. [CrossRef] [Google Scholar] [Publisher Link]

[24] J. F. Witte et al., "A Current-Feedback Instrumentation Amplifier with 5 μV Offset for Bidirectional High-Side Current-Sensing," *2008 IEEE International Solid-State Circuits Conference - Digest of Technical Papers*, San Francisco, CA, USA, pp. 574-596, 2008. [CrossRef] [Google Scholar] [Publisher Link]

[25] Joshua T. Ramdeo, and Viranjay M. Srivastava, "Prototype Design and Analysis of 4-Stage Operational-Amplifier using Double-Gate MOSFET," *International Journal of Engineering Trends and Technology*, vol. 71, no. 7, pp. 175-188, 2023. [CrossRef] [Publisher Link]

[26] J. Hinay Shelly, and B. Craige Shreen, "D Flip Flops for Linear Response Shift Register in CMOS Technology," *SSRG International Journal of VLSI & Signal Processing*, vol. 4, no. 3, pp. 16-20, 2017. [CrossRef] [Publisher Link]

[27] Wei-Song Wang et al., "Low-Power Instrumental Amplifier for Portable ECG," *2009 IEEE Circuits and Systems International Conference on Testing and Diagnosis*, Chengdu, China, pp. 1-4, 2009. [CrossRef] [Google Scholar] [Publisher Link]

[28] E. Sackinger, and W. Guggenbuhl, "A Versatile Building Block: The CMOS Differential Difference Amplifier," *IEEE Journal of Solid-State Circuits*, vol. 22, no. 2, pp. 287-294, 1987. [CrossRef] [Google Scholar] [Publisher Link]

[29] Rida S. Assaad, and Jose Silva-Martinez, "The Recycling Folded Cascode: A General Enhancement of the Folded Cascode Amplifier," *IEEE Journal of Solid-State Circuits*, vol. 44, no. 9, pp. 2535-2542, 2009. [CrossRef] [Google Scholar] [Publisher Link]

[30] F. Corsi, and C. Marzocca, "An Approach to the Analysis of the CMOS Differential Stage with Active Load and Single-Ended Output," *IEEE Transactions on Education*, vol. 46, no. 3, pp. 325-328, 2003. [CrossRef] [Google Scholar] [Publisher Link]

[31] Montree Kumngern, Tomasz Kulej, and Fabian Khateb, "31.3 nW, 0.5 V Bulk-Driven OTA for Biosignal Processing," *IEEE Access*, vol. 11, pp. 56516-56525, 2023. [CrossRef] [Google Scholar] [Publisher Link]